Investigation of the frequency shifts of 24 solar-like stars observed by *Kepler*

René Kiefer[1]
A. Schad[1] G. Davies[2] M. Roth[1]

July 13, 2016

Seismology of the Sun and the Distant Stars 2016

Joint TASC2 & KASC9 Workshop – SPACEINN & HELAS8 Conference

[1]Kiepenheuer-Institut für Sonnenphysik Freiburg
[2]School of Physics and Astronomy, University of Birmingham

Motivation

- For the Sun: Frequency shifts correlated with activity
- Better understand stellar dynamos and stellar activity, also important for study of planetary habitability

Motivation

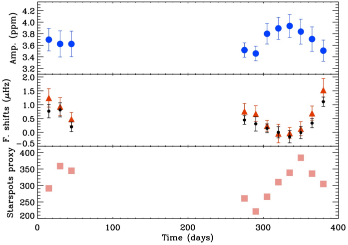

Detection of a stellar activity cycle in HD49933. From: García et al. (2010)

- For the Sun: Frequency shifts correlated with activity
- Better understand stellar dynamos and stellar activity, also important for study of planetary habitability
- HD49933: First asteroseismic detection of stellar cycle

Motivation

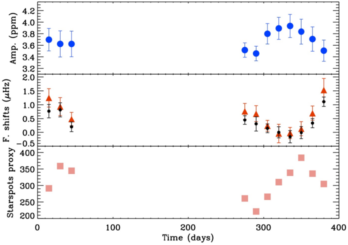

Detection of a stellar activity cycle in HD49933. From: García et al. (2010)

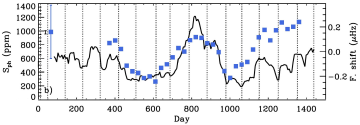

From: Salabert et al. (2016)

- For the Sun: Frequency shifts correlated with activity
- Better understand stellar dynamos and stellar activity, also important for study of planetary habitability
- HD49933: First asteroseismic detection of stellar cycle
- *Kepler* photometry, activity index S_{ph}

Data

- SC data of 24 solar-like stars, corrected and concatenated time series (Handberg and Lund, 2014)
- No strict selection criteria applied
- Length of data between 960 - 1147 days

Data

- SC data of 24 solar-like stars, corrected and concatenated time series (Handberg and Lund, 2014)
- No strict selection criteria applied
- Length of data between 960 - 1147 days

- Lomb-Scargle periodograms from 100(150) day long segments
- Shift of 50 days, 2(3) time overlap
- No oversampling

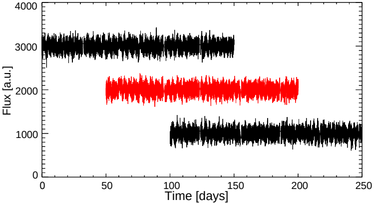

Cross-correlation

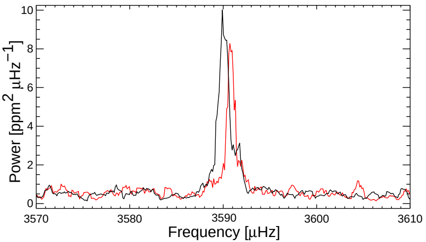

Section of LSP of 1st and 19th segment of KIC 8006161

- Choose frequency range, where peaks are visible in the periodogram

Cross-correlation

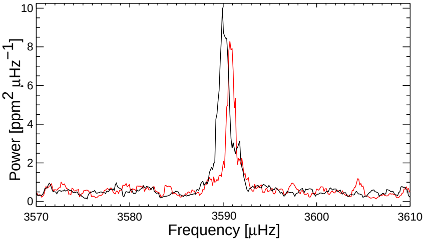

Section of LSP of 1st and 19th segment of KIC 8006161

- Choose frequency range, where peaks are visible in the periodogram

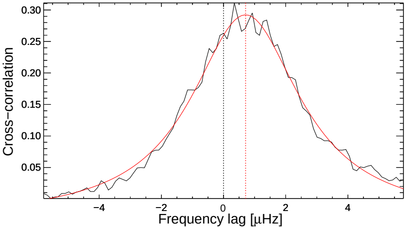

Cross-correlation of full range of p modes of KIC 8006161

- Fit Lorentzian to cross-correlation, convolution of two Lorentzians gives a Lorentzian
- Error estimation by resampling approach

Error estimation

- Resampling of the time series
- Draw 200 complex random series for each segment's PSD by:

$$\Re\{F_i^*(\nu_k)\} \sim \sqrt{\hat{S}_i(\nu_k)} \times N(0,1)$$
$$\Im\{F_i^*(\nu_k)\} \sim \sqrt{\hat{S}_i(\nu_k)} \times N(0,1)\,,$$

- Estimate $\hat{S}_i$ of the true unknown S_i obtained by smoothing the LSP, width depending on noise properties, mode widths
- Mean of 200 fits: Shift
- Standard deviation of 200 fits: Error

Consistency check

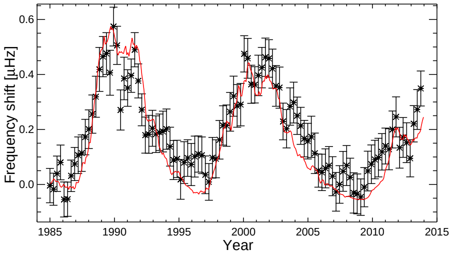

Black data points: Frequency shifts from Bison data (Davies et al., 2014).

Red line: Smoothed monthly sunspot number, from: WDC-SILSO, Royal Observatory of Belgium, Brussels.

- Frequency range: 1800-3800 μHz
- 200 days segments, 100 days shift, two-time overlap
- Frequency shift amplitude $0.62 \pm 0.06\,\mu$Hz
- In agreement with previous studies (e.g. Chaplin et al., 2007a)

KIC 8006161 aka Doris

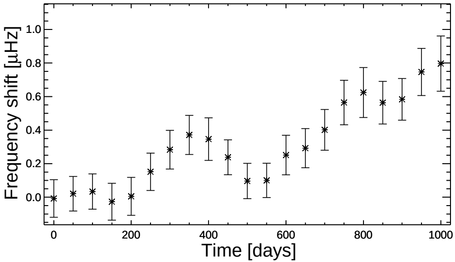

Frequency shifts from the full p-mode range 2800-4400 μHz

- Very similar to the Sun:
  $1.00 \pm 0.01\,\mathrm{M}_\odot$
  $0.93 \pm 0.01\,\mathrm{R}_\odot$
  $4.28 \pm 0.12\,\mathrm{Gyr}$, G8V
- Rotation period:
  $29.79 \pm 3.09\,\mathrm{d}$
- Shift amplitude:
  $0.84 \pm 0.19\,\mu$Hz
- Not covering a full cycle:
  $P_{\mathrm{cyc}} > 1147\,\mathrm{d}$

Citations on these values see Appendix

KIC 8006161 aka Doris

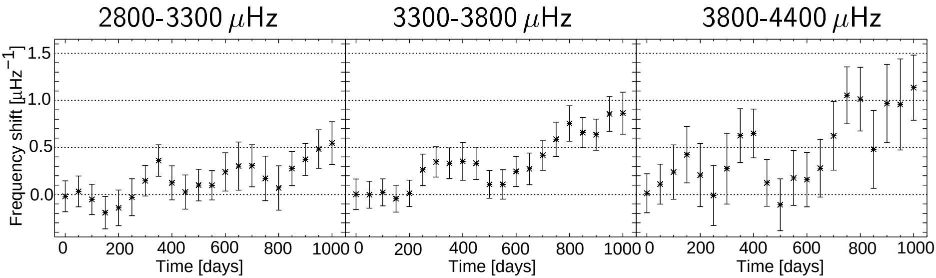

- Frequency shifts for three different frequency ranges
- Shifts, errors increase with frequency
- Frequency shift larger then for the Sun, even in the low frequency range, confirms S_{ph} measurements of García et al. (2014)

Out-of-sight but not hidden: KIC 10644253

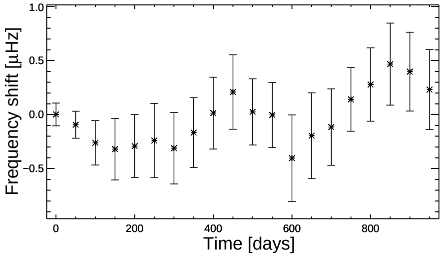

- Solar analog: $1.13 \pm 0.05\,\mathrm{M}_\odot$ $1.108 \pm 0.016\,\mathrm{R}_\odot$ $1.07 \pm 0.25\,\mathrm{Gyr}$, G0V
- Rotation period: $10.91 \pm 0.87\,\mathrm{d}$
- Shift amplitude: $0.895\,\mu$Hz
- Low inclination: $i = 23 \pm 6^\circ$

Out-of-sight but not hidden: KIC 10644253

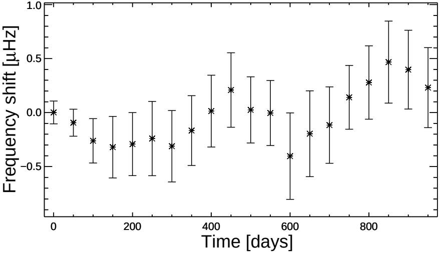

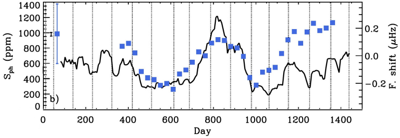

From: Salabert et al. (2016)

- Solar analog: $1.13 \pm 0.05\,\mathrm{M}_\odot$ $1.108 \pm 0.016\,\mathrm{R}_\odot$ $1.07 \pm 0.25\,\mathrm{Gyr}$, G0V
- Rotation period: $10.91 \pm 0.87\,\mathrm{d}$
- Shift amplitude: 0.895 μHz
- Low inclination: $i = 23 \pm 6^\circ$
- Discrepancy between photometric activity index S_{ph} and frequency shift
- Activity on the out-of-sight hemisphere?

Citations on these values see Appendix

The full sample

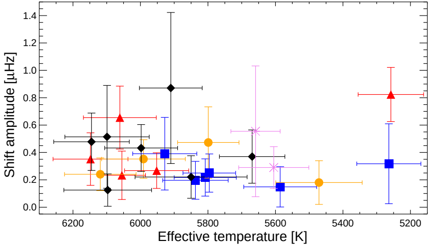

T < 4 Gyrs,

4 Gyrs < T < 5 Gyrs,

5 Gyrs < T < 6 Gyrs

6 Gyrs < T < 8 Gyrs

T > 8 Gyrs

The full sample

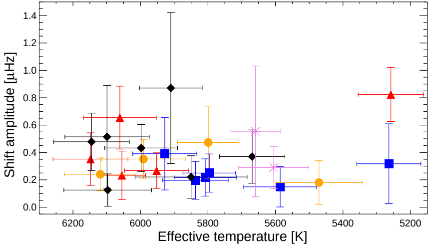

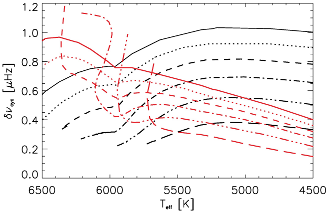

From: Karoff et al. (2009)

- Two proposed scalings for frequency shifts:
  - Proportional to strength of stellar activity $\Delta R'_{\mathrm{HK}}$ (Chaplin et al., 2007b, black lines)
  - Proportional to $\frac{R^{2.5}L^{0.25}}{M^2}\Delta R'_{\mathrm{HK}}$ (Metcalfe et al., 2007, red lines)

The full sample

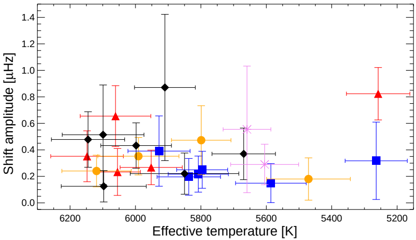

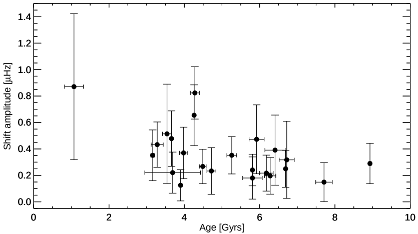

- Sample too small, errors too large
- Take full SC sample
- Use individual mode fitting to decrease error

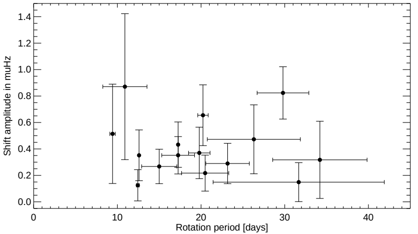

Summary

- We investigated the frequency shifts of 24 solar-like stars observed by *Kepler*
- 22 of them show significant (A/σ_A >1) frequency shifts
- KIC 8006161 shows strong shifts $\delta\nu = 0.84\,\mu$Hz
- KIC 8006161 cycle length >1147 days
- KIC 10644253 shows signs of activity on out-of-sight hemisphere
- No decision between different models for scaling of frequency shifts possible: more stars, smaller errors needed

- Paper submitted to A&A

Thank you for your attention!

References I

R. A. García, S. Mathur, D. Salabert, et al. CoRoT Reveals a Magnetic Activity Cycle in a Sun-Like Star. *Science*, 329:1032–, August 2010. doi: 10.1126/science.1191064.

D. Salabert, C. Régulo, R. A. García, et al. Magnetic variability in the young solar analog KIC 10644253. Observations from the Kepler satellite and the HERMES spectrograph. *A&A*, 589:A118, May 2016. doi: 10.1051/0004-6361/201527978.

R. Handberg and M. N. Lund. Automated preparation of Kepler time series of planet hosts for asteroseismic analysis. *Mon. Not. Roy. Astron. Soc.*, 445:2698–2709, December 2014. doi: 10.1093/mnras/stu1823.

G. R. Davies, W. J. Chaplin, Y. Elsworth, and S. J. Hale. BiSON data preparation: a correction for differential extinction and the weighted averaging of contemporaneous data. *Mon. Not. Roy. Astron. Soc.*, 441:3009–3017, July 2014. doi: 10.1093/mnras/stu803.

W. J. Chaplin, Y. Elsworth, B. A. Miller, G. A. Verner, and R. New. Solar p-Mode Frequencies over Three Solar Cycles. *Astrophys. J.*, 659:1749–1760, April 2007a. doi: 10.1086/512543.

RA García, T Ceillier, D Salabert, et al. Rotation and magnetism of kepler pulsating solar-like stars-Towards asteroseismically calibrated age-rotation relations. *A&A*, 572:A34, 2014.

C. Karoff, T. S. Metcalfe, W. J. Chaplin, et al. Sounding stellar cycles with Kepler - I. Strategy for selecting targets. *Mon. Not. Roy. Astron. Soc.*, 399:914–923, October 2009. doi: 10.1111/j.1365-2966.2009.15323.x.

W. J. Chaplin, Y. Elsworth, G. Houdek, and R. New. On prospects for sounding activity cycles of Sun-like stars with acoustic modes. *Mon. Not. Roy. Astron. Soc.*, 377:17–29, May 2007b. doi: 10.1111/j.1365-2966.2007.11581.x.

T. S. Metcalfe, W. A. Dziembowski, P. G. Judge, and M. Snow. Asteroseismic signatures of stellar magnetic activity cycles. *Mon. Not. Roy. Astron. Soc.*, 379:L16–L20, July 2007. doi: 10.1111/j.1745-3933.2007.00325.x.

S. Mathur, T. S. Metcalfe, M. Woitaszek, et al. A Uniform Asteroseismic Analysis of 22 Solar-type Stars Observed by Kepler. *Astrophys. J.*, 749:152, April 2012. doi: 10.1088/0004-637X/749/2/152.

References II

T. S. Metcalfe, O. L. Creevey, G. Doğan, et al. Properties of 42 Solar-type Kepler Targets from the Asteroseismic Modeling Portal. *Astrophys. J. Suppl.*, 214:27, October 2014. doi: 10.1088/0067-0049/214/2/27.

D. Huber, V. Silva Aguirre, J. M. Matthews, et al. Revised Stellar Properties of Kepler Targets for the Quarter 1-16 Transit Detection Run. *Astrophys. J. Suppl.*, 211:2, March 2014. doi: 10.1088/0067-0049/211/1/2.

J. Molenda-Żakowicz, S. G. Sousa, A. Frasca, et al. Atmospheric parameters of 169 F-, G-, K- and M-type stars in the Kepler field. *Mon. Not. Roy. Astron. Soc.*, 434:1422–1434, September 2013. doi: 10.1093/mnras/stt1095.

H. Bruntt, S. Basu, B. Smalley, et al. Accurate fundamental parameters and detailed abundance patterns from spectroscopy of 93 solar-type Kepler targets. *Mon. Not. Roy. Astron. Soc.*, 423: 122–131, June 2012. doi: 10.1111/j.1365-2966.2012.20686.x.

M. H. Pinsonneault, D. An, J. Molenda-Żakowicz, et al. A Revised Effective Temperature Scale for the Kepler Input Catalog. *Astrophys. J. Suppl.*, 199:30, April 2012. doi: 10.1088/0067-0049/199/2/30.

A. McQuillan, T. Mazeh, and S. Aigrain. Stellar Rotation Periods of the Kepler Objects of Interest: A Dearth of Close-in Planets around Fast Rotators. *Astrophys. J. Lett.*, 775:L11, September 2013. doi: 10.1088/2041-8205/775/1/L11.

R. A. García, T. Ceillier, D. Salabert, et al. Rotation and magnetism of Kepler pulsating solar-like stars. Towards asteroseismically calibrated age-rotation relations. *A&A*, 572:A34, December 2014. doi: 10.1051/0004-6361/201423888.

A. McQuillan, T. Mazeh, and S. Aigrain. Rotation Periods of 34,030 Kepler Main-sequence Stars: The Full Autocorrelation Sample. *Astrophys. J. Suppl.*, 211:24, April 2014. doi: 10.1088/0067-0049/211/2/24.

Additional slides

Data of the time series and the periodograms

KIC	Data coverage*	Length of data (d)	Length of segment (d)	Frequency range (μHz)
3632418	5-17.2	1147	150	700-1700
3656476	7-17.2[a]	960	150	1500-2500
4914923	7-17.2	960	150	1350-2300
5184732	7-17.2	960	100	1400-2700
6106415	6-16[b]	1018	150	1550-3100
6116048	5-17.2	1147	150	1550-2600
6603624	5-17.2	1147	100	1900-3000
6933899	5-17.2	1147	150	1000-1800
7680114	7-17.2[c]	960	150	1350-2100
7976303	5-17.2	1147	150	550-1300
8006161	5-17.2	1147	100	2800-4400
8228742	5-17.2	1147	100	800-1600
8379927	5-17.2	1147	150	2100-3700
8760414	5-17.2	1147	150	1950-3000
9025370	5-17.2	1147	100	2550-3450
9955598	5-17.2	1147	150	3000-4100
10018963	5-17.2	1147	100	650-1500
10516096	7-17.2[d]	960	100	1200-1900
10644253	5-17.2	1147	150	2450-3350
10963065	5-15[e]	1027	150	1700-2700
11244118	5-17.2	1147	100	1000-1800
11295426	5-17.2	1147	150	1800-2400
12009504	5-17.2	1147	100	1400-2300
12258514	5-17.2	1147	150	1050-2100

* Data coverage indicated in *Kepler* quarters. Missing quarters: [a] Q10, Q14; [b] Q9, Q13; [c] Q6, Q7.2, Q10; [d] Q10.1; [e] Q8, Q9, Q12

Amplitudes of frequency shifts

KIC	A (0.1μHz)	σ_A (0.1μHz)	A/σ_A	KIC	A (0.1μHz)	σ_A (0.1μHz)	A/σ_A
3632418	3.77	1.75	2.16	8228742	6.24	2.41	2.59
3656476	1.33	1.37	0.97	8379927	4.14	1.69	2.45
4914923	2.04	1.34	1.53	8760414	2.11	1.42	1.49
5184732	3.55	1.86	1.91	9025370	5.28	4.74	1.11
6106415	2.33	1.73	1.34	9955598	2.89	3.04	0.95
6116048	3.61	1.51	2.40	10018963	4.41	2.30	1.92
6603624	1.73	1.54	1.13	10516096	4.19	2.38	1.76
6933899	1.89	1.27	1.49	10644253	8.95	6.41	1.40
7680114	4.44	2.48	1.79	10963065	1.38	1.16	1.19
7976303	2.38	1.28	1.85	11244118	3.06	1.62	1.89
8006161	8.35	1.88	4.44	11295426	2.38	1.56	1.52
low	7.39	2.85	2.59	12009504	5.04	3.54	1.42
mid	8.52	1.93	4.42	12258514	2.59	1.31	1.97
high	12.44	4.42	2.81				

Tables of stellar parameters

KIC	R [$R_\odot$]	σ_R [$R_\odot$]	M [$M_\odot$]	σ_M [$M_\odot$]	Age [Gyr]	$\sigma_{\mathbf{Age}}$ [Gyr]	Reference
3632418	1.84	0.01	1.28	0.01	3.16	0.05	(1)
3656476	1.32	0.03	1.09	0.01	7.71	0.22	(1)
4914923	1.37	0.05	1.1	0.01	6.18	0.18	(1)
5184732	1.36	0.01	1.25	0.01	3.98	0.11	(1)
6106415	1.24	0.01	1.12	0.02	4.72	0.12	(1)
6116048	1.26	0.01	1.12	0.02	5.26	0.13	(1)
6603624	1.15	0.01	1.01	0.01	5.81	0.26	(1)
6933899	1.58	0.01	1.1	0.01	6.28	0.15	(1)
7680114	1.45	0.03	1.19	0.01	5.92	0.2	(1)
7976303	2.03	0.05	1.17	0.02	5.81	0.03	(1)
8006161	0.93	0.01*	1.00	0.01	4.28	0.12	(1)
8228742	1.84	0.01	1.31	0.01	4.26	0.02	(1)
8379927	1.11	0.02	1.09	0.03	3.28	0.16	(1)
8760414	1.01	0.004	0.78	0.01	3.69	0.74	(2)
9025370	0.960	$^{+0.04}_{-0.03}$	0.83	$^{+0.12}_{-0.06}$	13.1	$^{+3.4}_{-5.4}$	(3), (4)
9955598	0.883	0.008	0.89	0.02	6.72	0.2	(2)
10018963	1.91	0.01	1.17	0.01	3.66	0.02	(1)
10516096	1.42	0.03	1.12	0.03	6.41	0.27	(1)
10644253	1.108	0.016	1.13	0.05	1.07	0.25	(2)
10963065	1.2	0.09	1.03	0.03	3.9	0.04	(1)
11244118	1.55	0.01	1.01	0.01	8.93	0.04	(1)
11295426	1.243	0.019	1.079	0.051	6.69	—	(3), (4)
12009504	1.43	0.04	1.26	0.02	3.54	0.12	(1)
12258514	1.59	0.01	1.22	0.01	4.49	0.09	(1)

*In Mathur et al. (2012) this value is $0.00 R_\odot$. References: (1) Mathur et al. (2012),(2) Metcalfe et al. (2014), (3) Huber et al. (2014), (4) AMP

KIC	Spectral type	T_{eff} [K]	$\sigma_{T_{\mathrm{eff}}}$ [K]	Reference	P_{rot} [d]	$\sigma_{P_{\mathrm{rot}}}$ [d]	Reference
3632418	F6IV	6148	111	(1)	12.591	0.036	(5)
3656476	G5IV	5586	108	(1)	31.67	3.53	(6)
4914923	G1.5V	5808	92	(1)	20.49	2.82	(6)
5184732	G4V	5669	97	(1)	19.79	2.43	(6)
6106415	G0	6055	70	(2), (3)	—	—	—
6116048	F9IV-V	5991	124	(1)	17.26	1.96	(6)
6603624	G8IV-V	5471	128	(1)	—	—	—
6933899	G0.5IV	5837	97	(1)	—	—	—
7680114	G0V	5799	91	(1)	26.31	1.86	(6)
7976303	F8V	6119	106	(1)	—	—	—
8006161	G8V	5258	97	(1)	29.79	3.09	(6)
8228742	F9IV-V	6061	108	(1)	20.23	2.16	(6)
8379927	F9IV-V	5998	108	(1)	17.25	0.026	(7)
8760414	G0IV	5850	166	(1)	—	—	—
9025370	F8	5659	73	(2), (4)	—	—	—
9955598	K0V	5264	95	(1)	34.20	5.64	(6)
10018963	F6IV	6145	112	(1)	—	—	—
10516096	F9IV-V	5928	95	(1)	—	—	—
10644253	G0V	5910	93	(1)	10.91	0.87	(6)
10963065	F8V	6097	130	(1)	12.444	0.172	(5)
11244118	G5IV	5605	104	(1)	23.17	3.89	(6)
11295426	—	5796	78	(4)	—	—	—
12009504	F9IV-V	6099	125	(1)	9.426	0.327	(7)
12258514	G0.5IV	5952	95	(1)	15.00	1.84	(6)

References: (1) Molenda-Żakowicz et al. (2013), (2) SIMBAD entry without reference, (3) Bruntt et al. (2012), (4) Pinsonneault et al. (2012), (5) McQuillan et al. (2013), (6) García et al. (2014), (7) McQuillan et al. (2014)

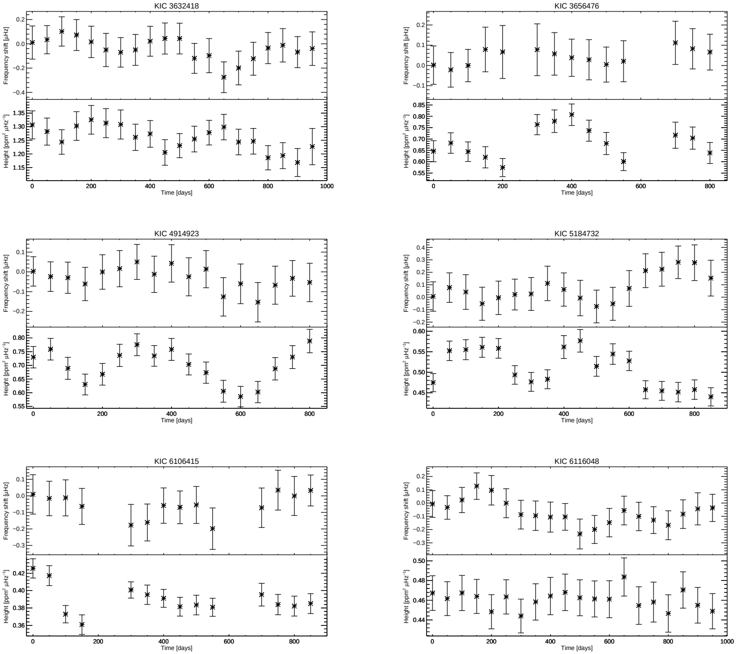

KIC 3632418
KIC 3656476
KIC 4914923
KIC 5184732
KIC 6106415
KIC 6116048
Frequency shift [μHz]
Height [ppm^2 μHz^{-1}]
Time [days]

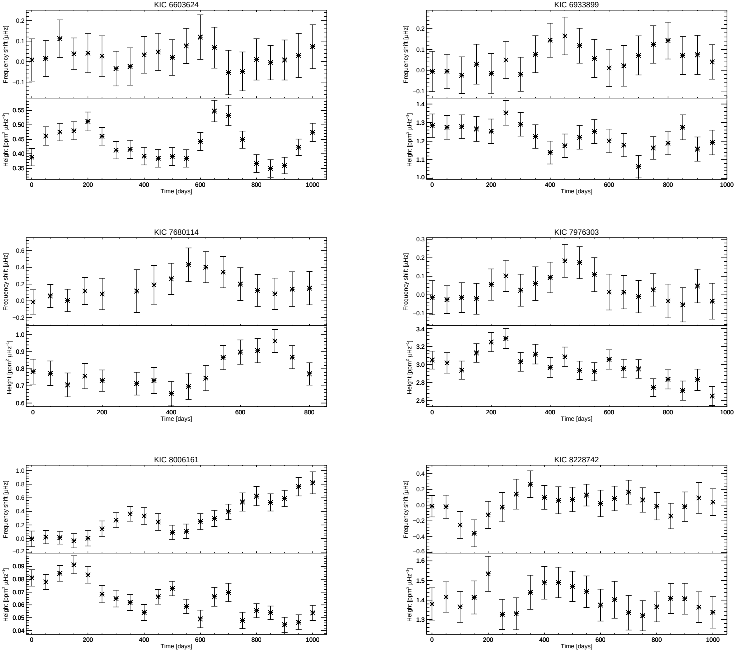
KIC 6603624
Frequency shift [μHz]
Height [ppm² μHz⁻¹]
Time [days]
KIC 6933899
Frequency shift [μHz]
Height [ppm² μHz⁻¹]
Time [days]
KIC 7680114
Frequency shift [μHz]
Height [ppm² μHz⁻¹]
Time [days]
KIC 7976303
Frequency shift [μHz]
Height [ppm² μHz⁻¹]
Time [days]
KIC 8006161
Frequency shift [μHz]
Height [ppm² μHz⁻¹]
Time [days]
KIC 8228742
Frequency shift [μHz]
Height [ppm² μHz⁻¹]
Time [days]

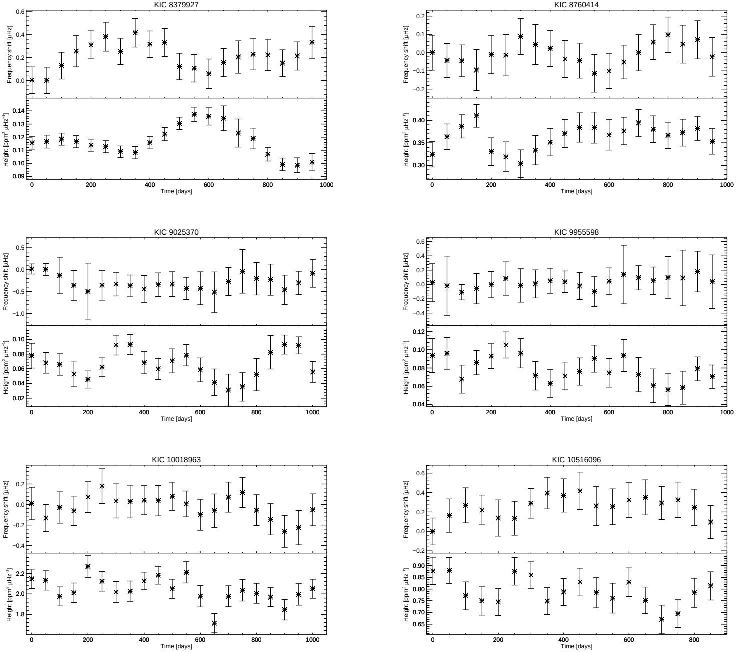
KIC 8379927
KIC 8760414
KIC 9025370
KIC 9955598
KIC 10018963
KIC 10516096
Frequency shift [μHz]
Height [ppm² μHz⁻¹]
Time [days]

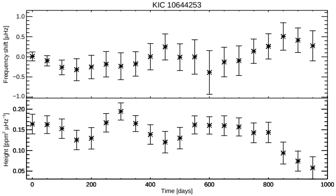
KIC 10644253
Frequency shift [μHz]
Height [ppm² μHz⁻¹]
Time [days]

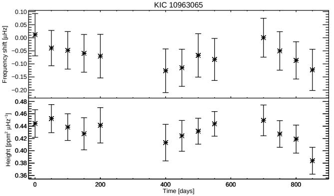
KIC 10963065
Frequency shift [μHz]
Height [ppm² μHz⁻¹]
Time [days]

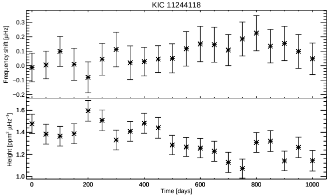
KIC 11244118
Frequency shift [μHz]
Height [ppm² μHz⁻¹]
Time [days]

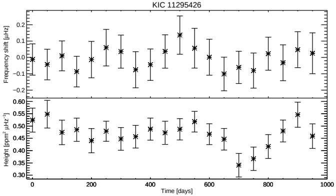
KIC 11295426
Frequency shift [μHz]
Height [ppm² μHz⁻¹]
Time [days]

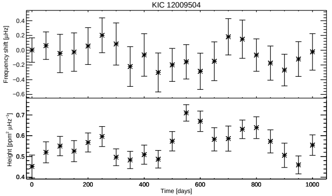
KIC 12009504
Frequency shift [μHz]
Height [ppm² μHz⁻¹]
Time [days]

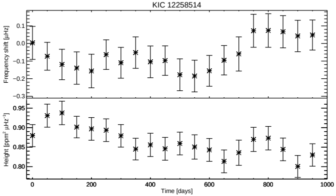
KIC 12258514
Frequency shift [μHz]
Height [ppm² μHz⁻¹]
Time [days]

Frequency Shifts and Mode Heights

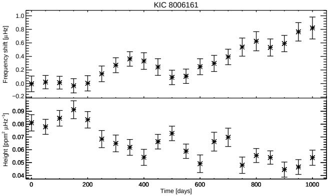

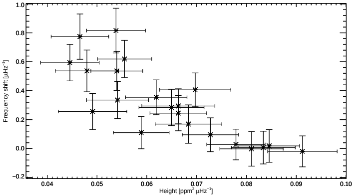

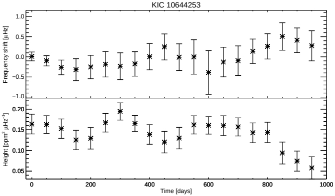

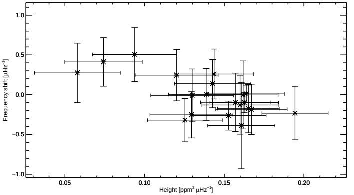

Frequency Shifts and Mode Heights